This project has received funding from the European Union's Seventh Programme for research, technological development and demonstration under grant agreement No [308417]".

New Directions in Seismic Hazard Assessment through Focused Earth Observation in the Marmara Supersite

Grant Agreement Number: 308417
co-funded by the European Commission within the Seventh Framework Programme
THEME [ENV.2012.6.4-2]
[Long-term monitoring experiment in geologically active regions of Europe prone to natural hazards: the Supersite concept]

Deliverable 2.4

Report on interpretative models correlating gas, crustal deformation and seismic activity

Project Start Date	1 November 2012
Project Duration	36 months
Project Coordinator /Organization	Nurcan Meral Özel / KOERI
Work Package Number	WP 2
Deliverable Name/ Number	D 2.4
Due Date Of Deliverable	29 February 2016
Actual Submission Date	29 April 2016
Organization/Author (s)	INGV / F. Italiano, A. Sciarra, L. Pizzino; GFZ / H. Woith, MAM / C. Seyis, KOU / D. Çaka

Dissemination Level		
PU	Public	
PP	Restricted to other programme participants (including the Commission)	
RE	Restricted to a group specified by the consortium (including the Commission)	
CO	Confidential, only for members of the consortium (including the Commission)	

TABLE OF CONTENTS

List of tables

List of figures

1 INTRODUCTION

Earthquakes may affect the fluid inventory co- and post-seismically inducing changes in water level in wells (Wang and Manga, 2010), in temperature (Mogi et al., 1989) and/or chemical composition of groundwaters (Skelton et al., 2014; Woith et al., 2003), in the flow-rate of gas discharges (Heinicke et al., 2006) and in their chemical and isotopic composition (Italiano et al., 2001, 2004, 2005, Hilton, 2007; Mutlu et al., 2012). Precursory changes have been proposed by many authors, but only few case studies made it into the IASPEI list of potential precursors. Among the very few "accepted" cases is one related to water level variations before the 1985 Kettleman Hills earthquake (Roeloffs and Quilty, 1997) and one related to radon variations before the 1978 Izu-Oshima-Kinkai earthquake (Wakita, 1981). Reviews on more recent hydrogeochemical presursors are provided by (Hartmann and Levy, 2005; Ingebritsen and Manga, 2014; Toutain and Baubron, 1999; Woith, 2015).

The relationship between fluids and seismogenesis has been approached collecting geochemical data of local significance and evaluating them in geochemical interpretative models of fluid circulation within the crust (e.g. Italiano et al., 2001, 2004, 2005).

As the fluids have high mobility migrating through fractures and faults and are fast carriers of information on the physico-chemical conditions at depth, they are able to reveal modifications in the equilibrium conditions at depth. Fluids may develop high pore pressures at depth capable to reduce the effective frictional strength of rocks; see (Sibson, 1992) for an in-depth discussion of fluid pressure cycles.

Our methodological approach aims to understand the genesis of the fluids, the components, the mixing proportions among various end-member components, as well as the thermodynamic equilibrium conditions at depth.

The geodynamic (geological setting, tectonics, seismicity) context of the area deeply influences the composition and the behavior of the fluids in terms of both chemical and isotopic composition as shallow-originated fluids usually mix with fluids coming from different depth levels of the crust and/or from the upper mantle. Such fluid mixing may change with the time due to both, seasonal variations and seismogenic processes (stress accumulation, deformation, strain release). Within the main frame of MARSITE project we followed a monitoring strategy focussed on the evaluation of potential indicators of the development of seismo-genesis and its impact on the circulating fluids. The seismic activity recorded during the time interval of the project is mainly located on the different branches of the NAFZ. We extracted the events marked by M>4 to carry out a preliminary check on the influence of ruptures (Fig. 1) on the fluids behaviour. A model of fluids circulation and interactions with the strike-slip North Anatolian Fault is proposed. The model accounts for the geochemical features of the fluids collected and analyzed as well as for the information provided by the soil degassing and continuous monitoring activity.

1.1 Seismicity

The earthquake catalogue built up during the MARSite project combined the seismology stations run by four different institutions (KOERI, TUBITAK, KOU and GFZ) in one single data-base (MARSite Main Server located at KOERI). About 5500 earthquakes ($0.5 \leq M_L \leq 5.5$) occurred between November 2012 and February 2016 (see plot on Figure 1).

The highest seismicity rate has been recorded along the Main Marmara Fault (western segment of North Anatolian Fault in Marmara Sea). A significant seismic activity occurred over the fault segments located in southern Marmara sea (Gemlik Gulf, Manyas, Yenice, Gönen). The high number of earthquakes in Saroz Gulf (northwest of Çanakkale city) depicts the aftershock activity of 24 May 2014 North Aegean Earthquake (M_w=6.9) (Figure 1).

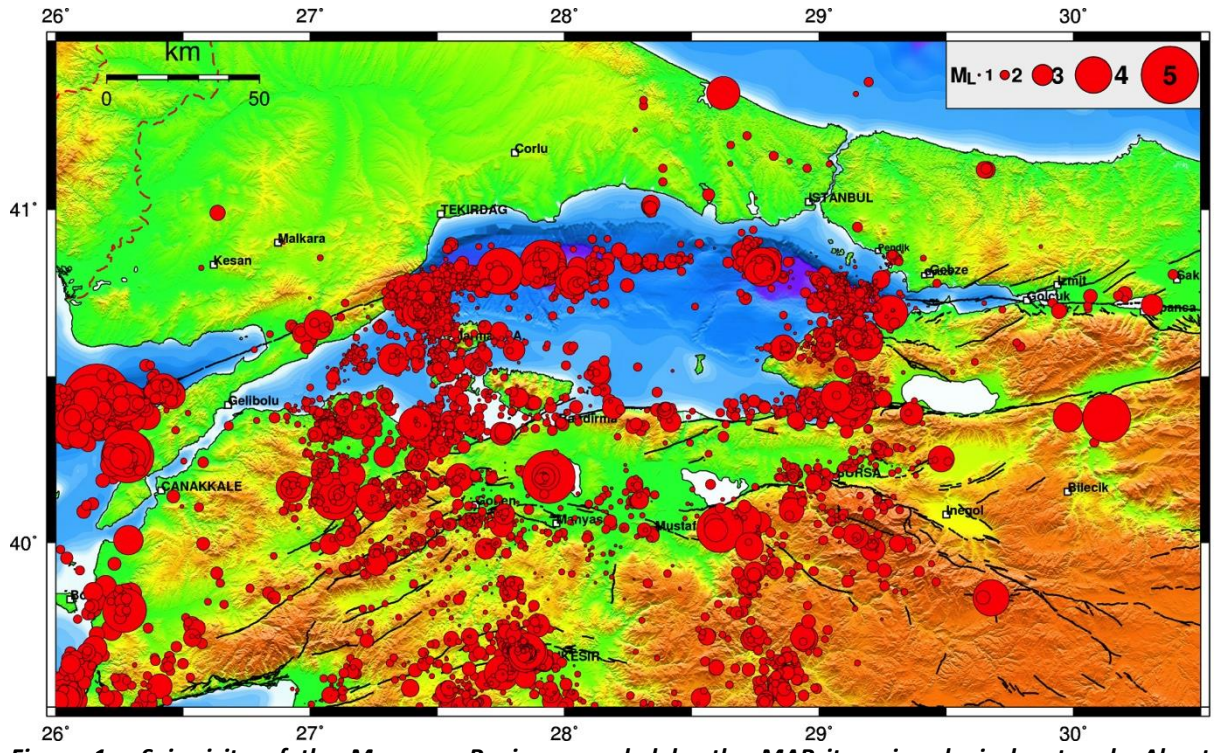

Figure 1 - Seismicity of the Marmara Region recorded by the MARsite seismological network. About 5500 earthquakes occurred in the MARSite project period.

We extracted the events marked by M>4 from the catalogue to check the positioning of the epicentral location with respect to the geochemical monitoring stations. Figure 2 plots together the selected events as well as the geochemical monitoring stations. The aim is to verify possible interactions of the occurred seismic shocks with the fluids expulsion and fluids behaviour.

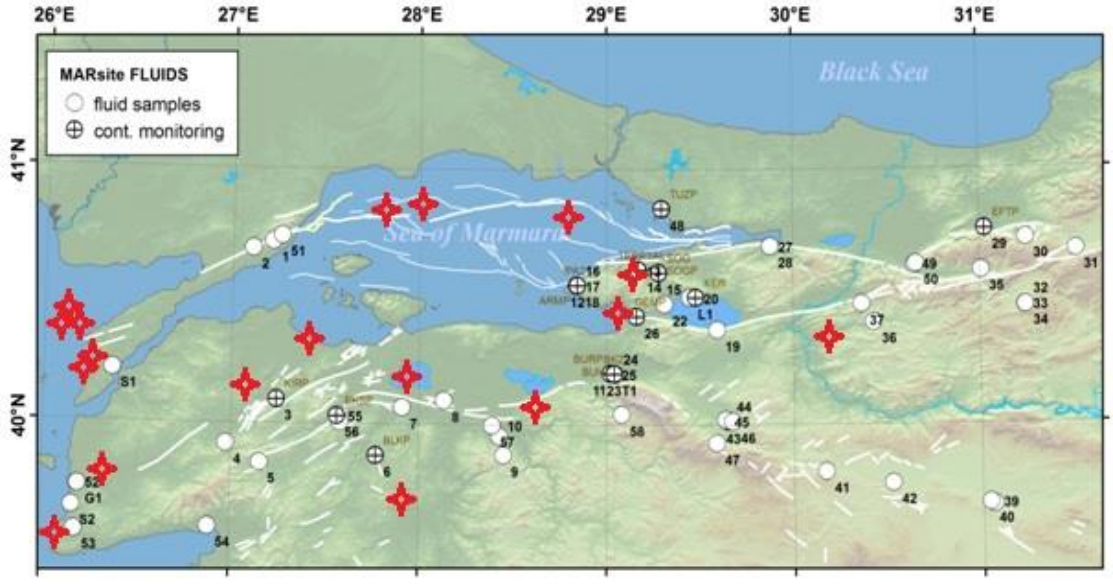

Figure 2 -Distribution of the epicenters for $M_L \geq 4.0$ earthquakes (red marks) recorded over in the Marmara area between 01.11.2012 and 29.02.2016. The location of the sampling sites is shown (white circles) as well as that of continuous groundwater monitoring stations (crossed circles).

The geochemical data presented in detail in D2.3 are hereafter discussed in terms of interactions with the faults and the faulting activity. The fluids/faults relationships can be well constrained by a deep investigation on the origin, interactions and temporal changes of the geochemical features of the fluids circulating over the different sectors of the NAFZ.

1.2 Gas geochemistry

The analytical results of the gases from 25 bubbling and 45 dissolved gases show that the gases released at the monitoring sites are a mixture of two end-members: one dominated by N_2 and the other dominated by CO_2. All the gases collected at the monitoring stations, including dissolved and bubbling samples plot along a mixing line between the two gases at different extents. Figure plots the CO_2-N_2 relationships due to two different, sometimes concomitants phenomena: mixing of fluids from the two different sources and Gas-Water-Interactions (GWI) leading to CO_2 dissolution and virtual enrichment in the gas phase of the less soluble gas species.

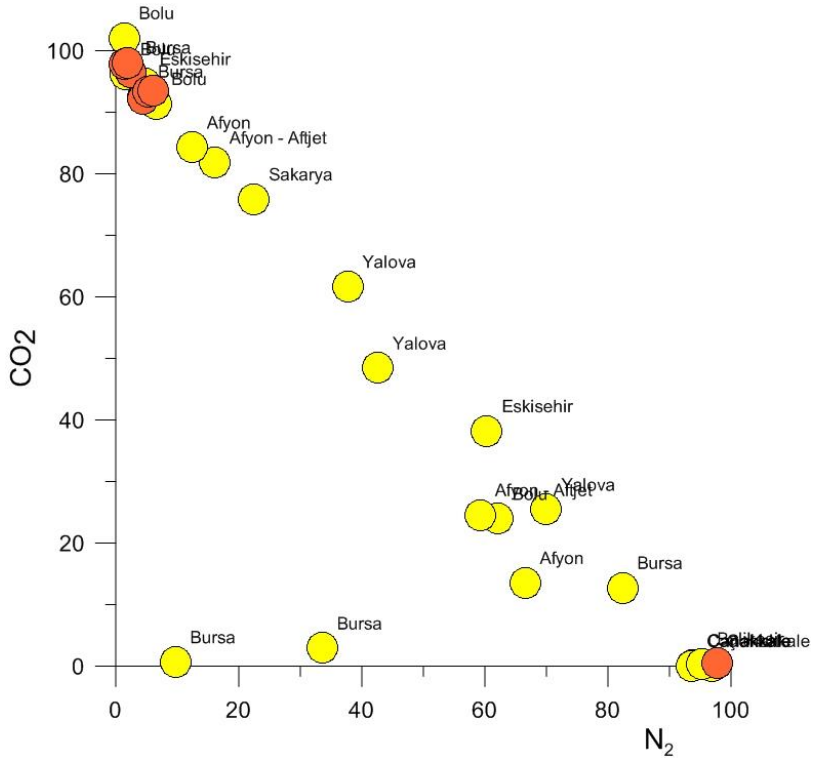

Figure 3 - Diagram N_2 vs. CO_2 that highlights the mixing at various extents between a CO_2- and a N_2-dominated gas phase.

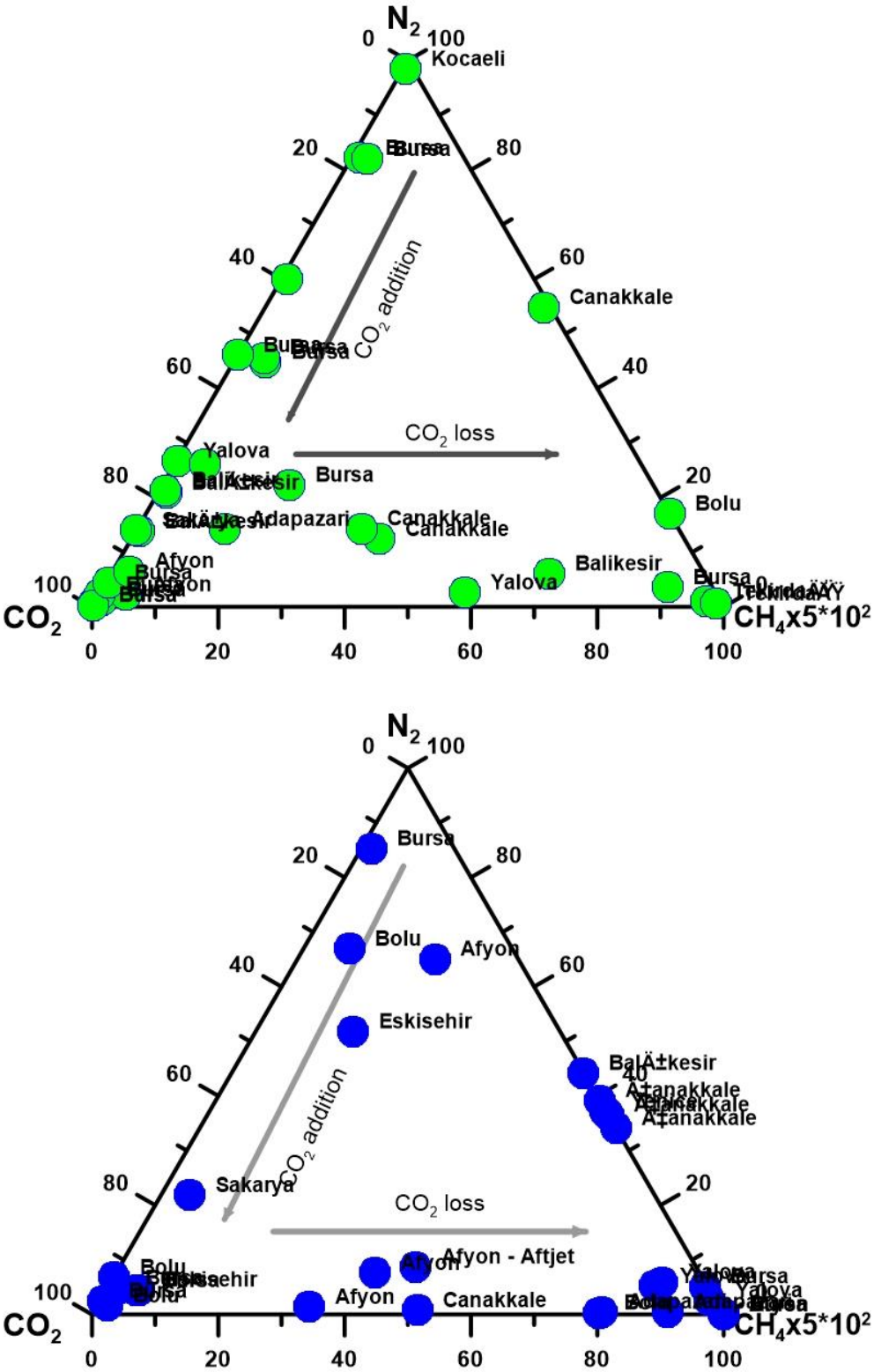

Figure 4 - CH_4-N_2-CO_2 ternary diagram for dissolved (above, green marks) and bubbling gases (below, blue dots). The arrows show the trends produced by the addition and dissolution of CO_2 to an atmospheric gas assemblage as well as addition of CH_4.

The CH_4-N_2-CO_2 ternary diagram (Figure 4 -) highlights the composition of the gases dissolved in the studied waters and released as free gas phase (bubbling gases). All of them are made of atmospheric-derived gas species (N_2) besides non-atmospheric gases (CO_2. CH_4). In both cases the graphs highlight the occurrence of CO_2 dissolution due to Gas Water Interactions (GWI) and CO_2 addition due to natural upraising of deep originated CO_2-dominated volatiles. CH_4 is present in significant concentration only at the northern shore of the Iznik Lake.

1.2.1 Helium isotopes

The isotopic composition of helium is always used to constrain the origin of a gas phase. The samples collected over the Marmara area underwent the analytical determination of the $^3He/^4He$ ratios. The helium isotopic data coupled with the chemical composition can provide a wide range of useful information to better understand the relationships of the circulating fluids with the different segments of the North Anatolian Fault Zone.

The analytical results of both dissolved and bubbling gases are listed in tables 1 and 2, respectively. Besides the $^4He/^{20}Ne$ ratios and the isotopic composition of carbon (as total dissolved inorganic carbon in dissolved gases and carbon of CO_2 in bubbling gases) display values in the range of 0.2-2.07 R/Ra (Ra is the isotopic ratio in air; all the values are normalized to the atmospheric composition; Table 1).

Table 1 - Isotopic composition of helium and carbon (as TDIC) as well as $^4He/^{20}Ne$ ratios in the dissolved gases. n.a. = not analyzed; n.d = not determined; bdl: below detection limits.

sample ID	site ID	Date	Region	R/Ra	$^4He/^{20}Ne$	$\delta^{13}C_{TDIC}$
14/02	TR410	31/08/2014	Adapazari	0.64	24.31	n.a.
14/03	TR411	31/08/2014	Adapazari	0.62	0.52	1.35
14/14	TR415	03/09/2014	Balikesir	0.80	0.43	n.a.
14/13	TR046	03/09/2014	Balikesir	0.88	0.3	-1.45
13/06	TR389	04/09/2014	Balikesir	1.00	5.30	-0.85
13/07	TR390	30/05/2013	Balıkesir	0.52	3.85	-5.02
13/08	TR391	30/05/2013	Balıkesir	0.94	0.87	-2.02
13/33	TR009	05/06/2013	Bolu	1.40	0.51	n.a.
13/35	TR398	05/06/2013	Bolu	1.85	1.25	n.a.
13/36	TR399	05/06/2013	Bolu	0.62	1.17	n.a.
13/23	TR209	02/06/2013	Bursa	0.96	0.38	n.a.
13/26	TR230	03/06/2013	Bursa	0.67	0.94	n.a.
14/24	TR230	08/09/2014	Bursa	0.57	1.26	0.48
14/16	TR232	04/09/2014	Bursa	0.90	49.72	3.52

13/09	TR233	30/05/2013	Bursa	1.12	0.43	0.48
13/54	TR237	10/06/2013	Bursa	0.70	2.93	n.a.
13/53	TR240	10/06/2013	Bursa	0.94	0.43	n.a.
13/24	TR320	03/06/2013	Bursa	1.05	16.55	n.a.
14/23	TR320	08/09/2014	Bursa	0.43	22.25	2.91
13/11	TR322	30/05/2013	Bursa	1.18	0.41	-3.43
14/18	TR322	04/09/2014	Bursa	0.53	1.90	-3.19
13/19	TR361	02/06/2013	Bursa	0.85	0.42	-3.73
13/10	TR392	30/05/2013	Bursa	1.14	0.35	-1.43
14/17	TR392	03/06/2013	Bursa	0.94	0.35	n.a.
13/50	TR407	10/06/2013	Bursa	0.78	0.49	n.a.
14/19	TR416	05/09/2014	Bursa	0.84	1.19	2.84
13/25	TR396	03/06/2013	Bursa	0.67	0.72	n.a.
14/07	TR343	02/09/2014	Canakkale	0.87	18.22	-1.71
13/04	TR352	02/09/2014	Canakkale	0.83	0.33	-14.39
14/11	TR414	03/09/2014	Canakkale	0.46	2.59	-13.86
13/45	TR379	08/06/2013	Eskisehir	0.86	0.36	n.a.
13/46	TR403	09/06/2013	Eskisehir	0.94	0.36	n.a.
13/47	TR404	09/06/2013	Eskisehir	0.91	0.44	n.a.
13/01	TR357	01/09/2014	Ganos	0.75	0.31	-15.87
14/04	TR412	01/09/2014	Ganos	4.41	2.75	-2.75
14/01	TR225	31/08/2014	Istanbul	0.59	11.36	n.a.
13/28	TR226	04/06/2013	Kocaeli	0.52	4.12	n.a.
13/29	TR366	04/06/2013	Kocaeli	0.73	16.86	0.21
13/37	TR400	05/06/2013	Sakarya	0.68	0.53	n.a.
13/02	TR388	28/05/2013	Tekirdağ	2.07	0.43	n.a.
14/05	TR388	28/05/2013	Tekirdağ	0.94	0.34	-17.47
13/13	TR393	31/05/2013	Yalova	0.34	4.00	-6.47
13/17	TR394	01/06/2013	Yalova	0.34	1.91	0.64
13/12	TR215	31/05/2013	Yalova	0.87	0.29	1.52
13/14	TR222	31/05/2013	Yalova	0.7	0.65	0.67

Table 2 - Isotopic composition of helium, carbon (CO_2) as well as $^{4}He/^{20}Ne$ ratios in the bubbling gases. n.a. = not analyzed; n.d = not determined; bdl: below detection limits.

Sample ID	Site ID	Date	Province	R/Ra	$^{4}He/^{20}Ne$	$\delta^{13}C_{CO2}$

14/02	TR410	31/08/2014	Adapazari	0.63	345.91	-1.68
14/03	TR411	31/08/2014	Adapazari	0.64	896.82	-3.81
13/06	TR389	29/05/2013	Balıkesir	0.97	0.36	-17.23
13/32	TR025	04/06/2013	Bolu	0.98	0.37	-3.3
13/31	TR029	04/06/2013	Bolu	0.72	1	-4.2
13/34	TR397	04/06/2013	Bolu	0.95	0.37	-1.8
13/35	TR398	05/06/2013	Bolu	1.59	0.78	-5.2
13/20	TR208	04/09/2014	Bursa	1.17	15.53	-6.18
13/24	TR320	30/05/2013	Bursa	0.97	0.4	-5
13/10	TR392	02/06/2013	Bursa	0.47	1.28	-9.4
14/17	TR392	02/06/2013	Bursa	0.96	0.32	-14.35
13/21	TR380	03/06/2013	Bursa	n.a.	n.a.	-5.22
13/51	TR408	10/06/2013	Bursa	0.52	30.77	-3.7
13/52	TR409	10/06/2013	Bursa	0.52	10.08	-6.2
14/07	TR343	02/09/2014	Canakkale	1.54	47.66	0
13/04	TR352	29/05/2013	Çanakkale	0.18	24.79	n.a.
13/03	TR353	29/05/2013	Çanakkale	0.2	40.14	n.a.
14/10	TR413	29/05/2013	Çanakkale	0.18	4.44	n.a.
13/46	TR403	08/06/2013	Eskisehir	0.71	0.72	n.a.
13/47	TR404	08/06/2013	Eskisehir	0.66	23.65	-2.5
13/38	TR037	05/06/2013	Sakarya	0.11	18.25	-6.1
13/18	TR395	31/05/2013	Yalova	0.92	0.31	-1.6
13/12	TR215	01/06/2013	Yalova	0.2	90.28	-2.7
13/16	TR347	01/06/2013	Yalova	0.26	10.54	-1.1
13/05	TR349	03/09/2014	Yenice	0.17	11.01	-4.5

.

The $^{4}He/^{20}Ne$ ratio indicates the extent of the atmospheric contamination ($^{4}He/^{20}Ne$ in air = 0.318; in ASW = 0.267) while the helium isotopic ratio indicates the contribution from different sources marked by different $^{3}He/^{4}He$ ratios in terms of Ra values: air= 1Ra; crustal fluids = 0.05Ra; mantle (MORB-type) fluids = 8Ra. Figure 5 shows the isotopic composition of helium vs. the $^{4}He/^{20}Ne$ ratio. The curves on figure 5 represent mixings between air and crustal or mantle fluids with different end-members (values in figure). The samples show basically a crustal origin with mantle contribution at variable extents. The values highlight a contribution of mantle-type fluids at all the monitoring stations making the monitored sited potentially useful to observe changes in the crust-mantle mixing ratios due to tectonic pulses.

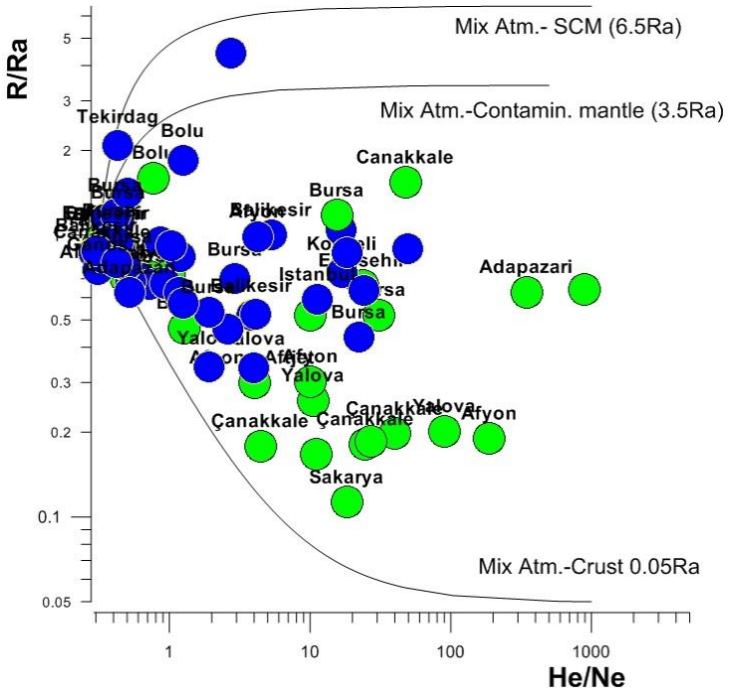

Figure 5 - Isotopic composition of helium R/Ra ratio vs. the $^{4}He/^{20}Ne$ ratio of MARsite fluid monitoring sites.

2 Fluids and crustal deformation

Crustal deformation may affect the circulation of fluids inside the crust due to changes of the porosity and fracturation during stress accumulation and stress release that in turn modify the permeability of the rocks.

Changes in the fluid circulation have been recorded during the MARsite project and they can be a consequence of periodical natural effects as seasonal rainfall or induced accidentally by human activities. Alternatively the changes can be a consequence of crustal deformation processes or, at least, of the ruptures in coincidence of seismic events.

A preliminary data analysis was performed on 34 stations of geochemical continuous monitoring belonging to the Tubitak and ARNET networks installed around the Marmara Sea Region. The open source software "R" was used to perform the data analysis. The Crosscorrelation diagrams between temperature and conductivity and Autocorrelation diagrams of the temperature data show periodical patterns for many stations . Autocorrelation diagrams of the conductivity data don't show any periodical patterns. The Classical Seasonal Decomposition (CSD) diagrams show various periodical patterns. Unfortunately they are too small (about 5 or 10 minutes) to be useful from a statistical point of view. Some stations show periodical patterns every 6 or 24 hours while patterns could be related to fault-fluid-stress relationships. An indication of the stress fields variation of could be suggested by the earthquakes (M_W>3) occurred over or close to the Marmara Sea region (the strongest earthquake had Mw~5.7). The non periodical patterns could be due to the stress variation caused by seismic shocks. This hypothesis should be verified performing other studies.

Examples are reported in figures 6, 7, 8.

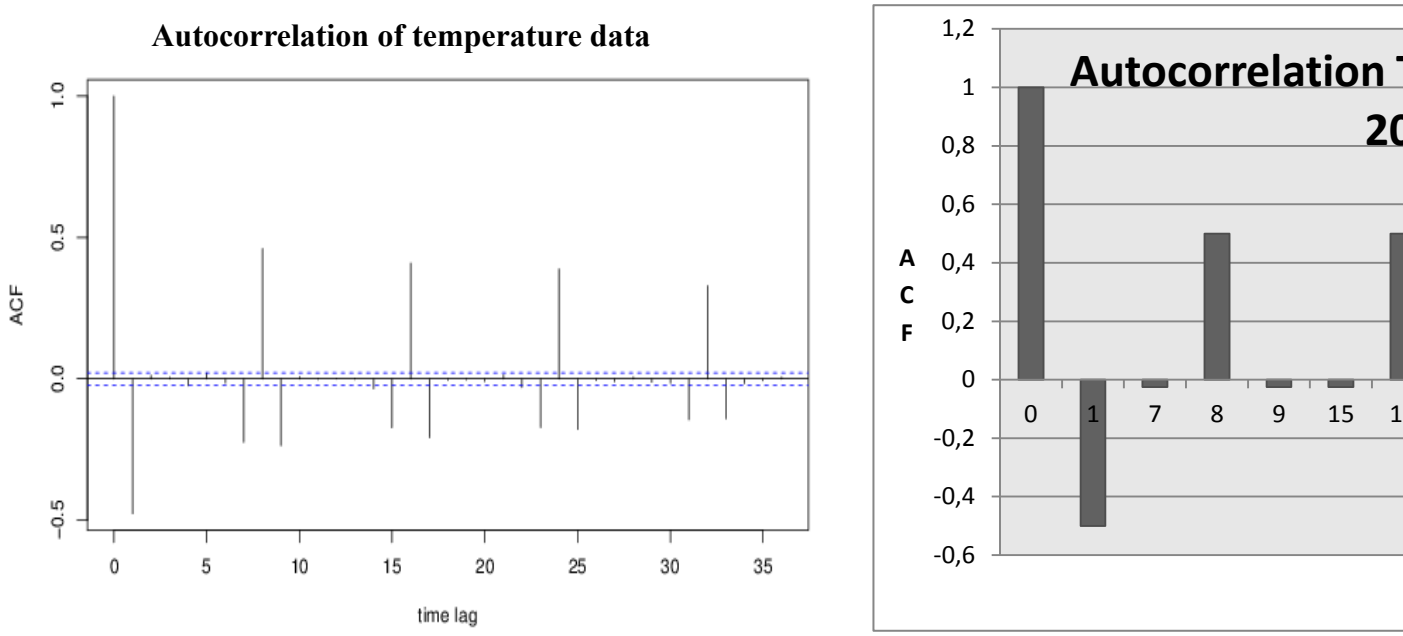

Figure 6 – Autocorrelation analysis of temperature data at the EFPT station showing the absence of periodical changes

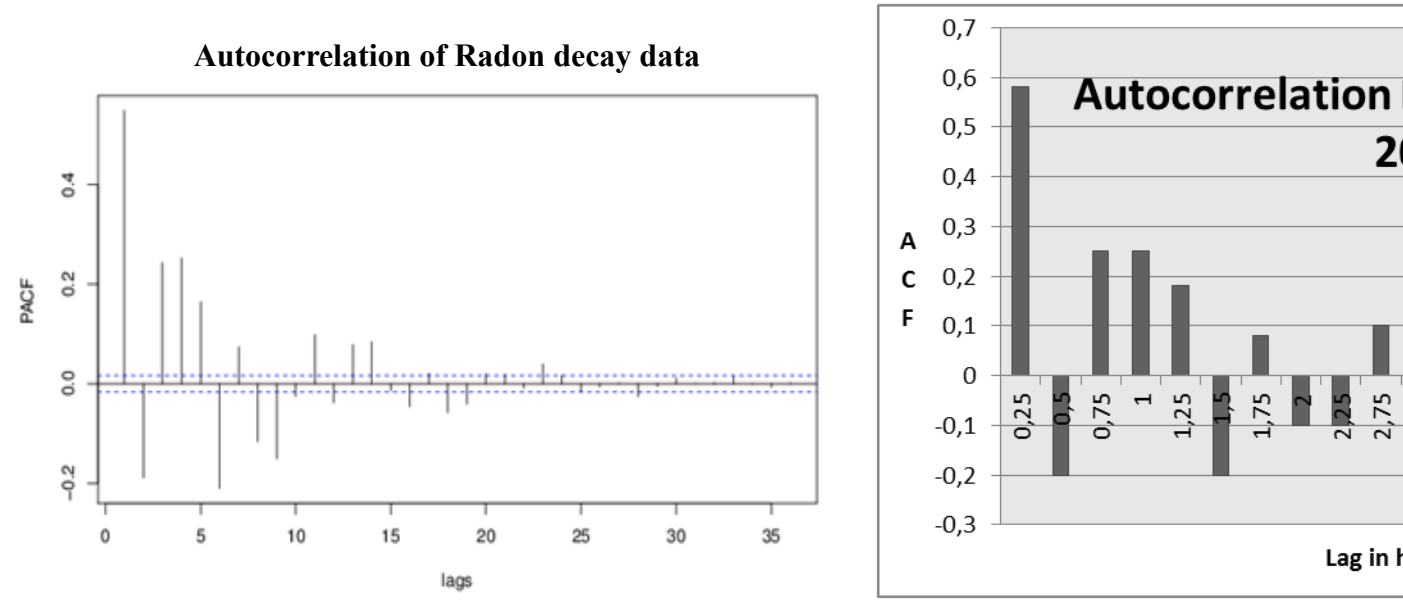

Figure 7– Autocorrelation analysis of Radon decay data at the GBZR station showing the existence of very short periodical changes (15 minutes)

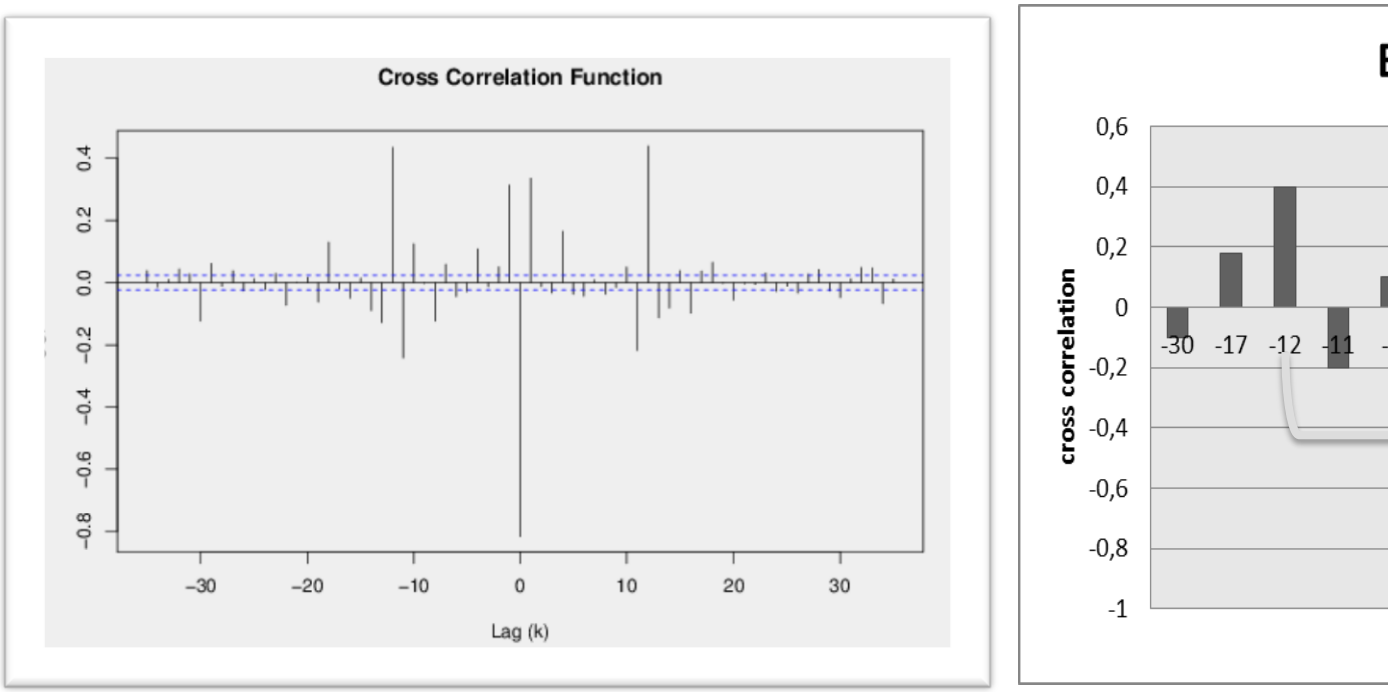

Figure 8– Cross correlation function at the BLKP station showing the existence of 4-24 hours periodical changes

Table 3 - Crosscorrelation patterns between temperature and electrical conductivity and autocorrelation patterns of radon decay estimated for the Tubitak and Arnet monitoring stations showing the absence of periodical patterns as well as the presence of periodical, tidal like periodical changes

Crosscorrelation between temperature and conductivity data		
Station name	Year	Periodic pattern
BLKP	2012	6 hours
"	2013	4-24 hours
"	2014	No pattern
BURP	2012	6 hours
"	2013	4-24 hours
"	2014	8 hours
EFTP	2012	4-8-14-24-48 hours
"	2013	No pattern
"	2014	6 hours
EKSP	2012	No pattern
"	2013	4-24 hours
"	2014	6-8 hours
HAMP	2012	6-8 hours
"	2013	6-44 -70 hours
"	2014	4-24 hours
KIRP	2012	4-6-8-24 hours
"	2013	4 hours
"	2014	No pattern
SOGP	2012	4 hours
"	2013	14 hours
"	2014	No pattern
TERP	2012	No pattern
"	2013	No pattern
"	2014	6-32 hours
TUZP	2012	4-6 hours
"	2013	4 hours
"	2014	4-6-8-10 hours

Autocorrelation of Radon decay data		
Station name	Year	Periodic pattern
ADAR	2012	No pattern
"	2013	No pattern
"	2014	No pattern
ARM5	2012	15 minutes
"	2013	No pattern
"	2014	15 minutes
ATCR	2012	15 minutes
"	2013	No pattern
"	2014	15 minutes
BLKR	2012	No pattern
"	2013	No pattern
"	2014	No pattern
CORB	2012	No pattern
"	2013	No pattern
"	2014	No pattern
DONR	2012	No pattern
"	2013	No pattern
"	2014	No pattern
EFTG	2012	No pattern
"	2013	No pattern
"	2014	No pattern
GBZR	2012	No pattern
"	2013	15 minutes
"	2014	15 minutes
HERR	2012	No pattern
"	2013	No pattern
"	2014	No pattern
KARR	2012	No pattern
"	2013	No pattern
"	2014	15 minutes

The behaviour of the fluids circulating in faulted areas is not directly related to the distance between the venting area and the epicentre. The coseismic crustal deformation postulated as to be assessable at any distance from the epicentral area by using the magnitude and the strain radius of the earthquakes (Dobrovolsky et al, 1979), as $\rho = 10^{0,43M}$ (where ρ (km) is strain radius and M is magnitude), seems to fail with the evidence that some earthquakes occurring not far away from a venting area do not induce any change in the circulating fluids and, contrastingly, events with epicenters far away from the venting areas provoke significant and sometimes permanent effects. Probably the main reason is that the theoretical approach by Dobrovolsky does not take into consideration the physical structure of the natural system that includes ruptures, fractures, faults and rocks of different nature and porosity. All of those systems react in different ways to external stress and result in different deformation rates either in coincidence of seismic events and during slow stress accumulation. Moreover, the fluids follow preferential paths namely paths with higher permeability and porosity. In case of seismic events, that is in case of a rupture of a fault segment, sudden changes in the permeability may occur and they are able to drive fluids migration more effectively than crustal deformation. An example has been recorded within the MARsite project activity over the area of Bursa. There was no anomaly before the 22.10.2014, M=4.5 earthquake, which occured at ~60 km to the east of the station. In contrast, there is a clear water temperature (wT) and water level (wL) increase before the 23.01.2015, M=4.5 earthquake, occurred at ~80 km southwest to

the station. We noticed the release of pressured gas while opening the wellhead. Thus, tentatively we propose that the changes in terms of water level and temperature (figure 12) could be a consequence of the rupture of a fault segment. The following images show examples of changes recorded at some monitoring stations potentially due to the occurrence of seismic shocks located on various segments of the NAFZ, thus at variable distances from the site of observation. It is easy to observe the absence of a direct relationship distance-intensity of the effect, namely distance-amplitude of the crustal deformations-amplitude of the induced effects.

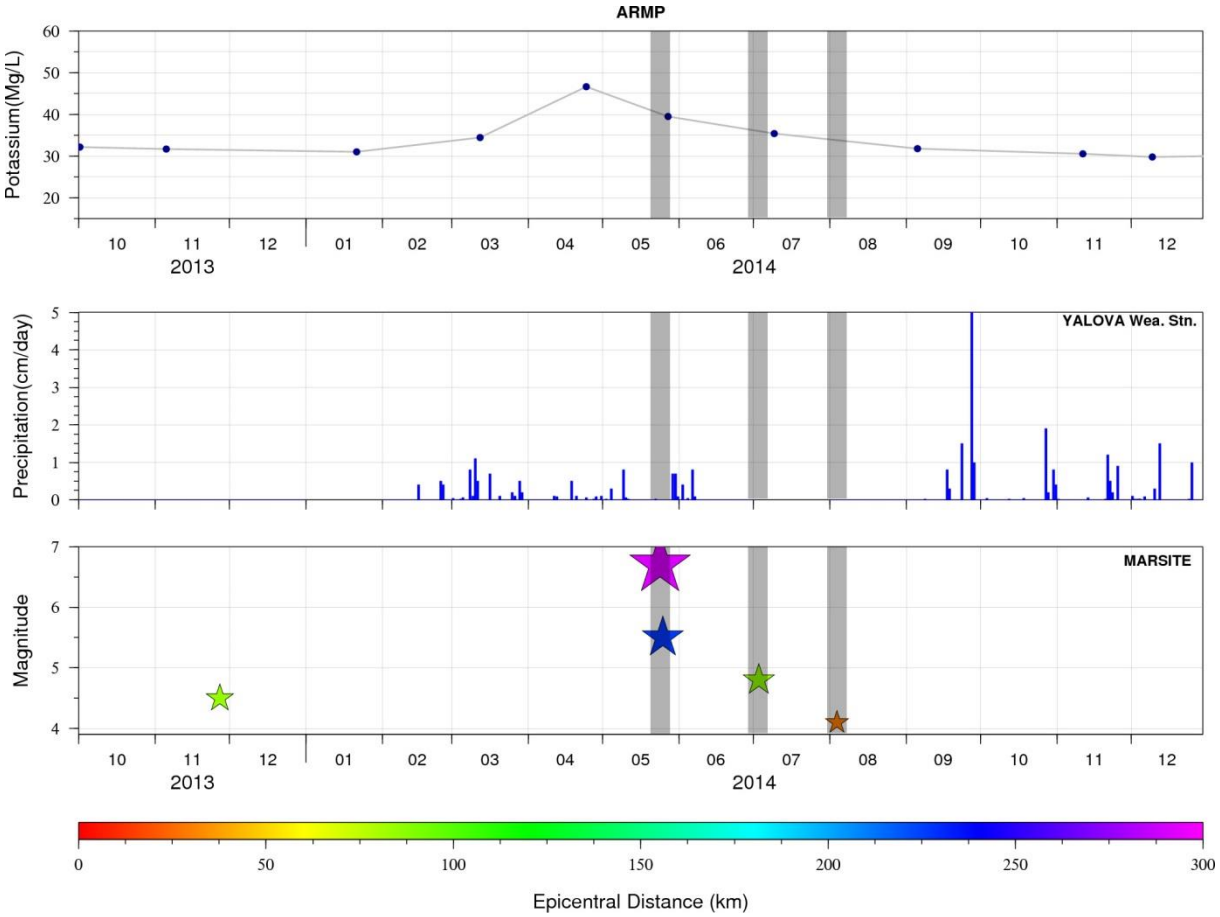

Figure 9. Detailed graph of ARMP (Armutlu, Yalova) groundwater stations Potassium graph, data from monthly sampled and laboratory measured anion-cation analysis. There is a clear potassium increase-decrease before the 24.05.2014, M=6.7 and 25.05.2014, M=5.5 earthquakes, which occur at ~220-300 km west to the station. The clear anomaly can also be related to the nearer 03.02.2014, M=4.8 (~80 km, southwest) or the very close 03.08.2014, M=4.1 (30km, east) earthquakes. It should also be noted that this station had given a very clear and several month long Sulfate anomaly before a suddenly appeared (November 2011) natural hydrogen sulfide rich gas discharge at the ~5 km southeast located Mecidiye Village (unpublished observation by TUBITAK).

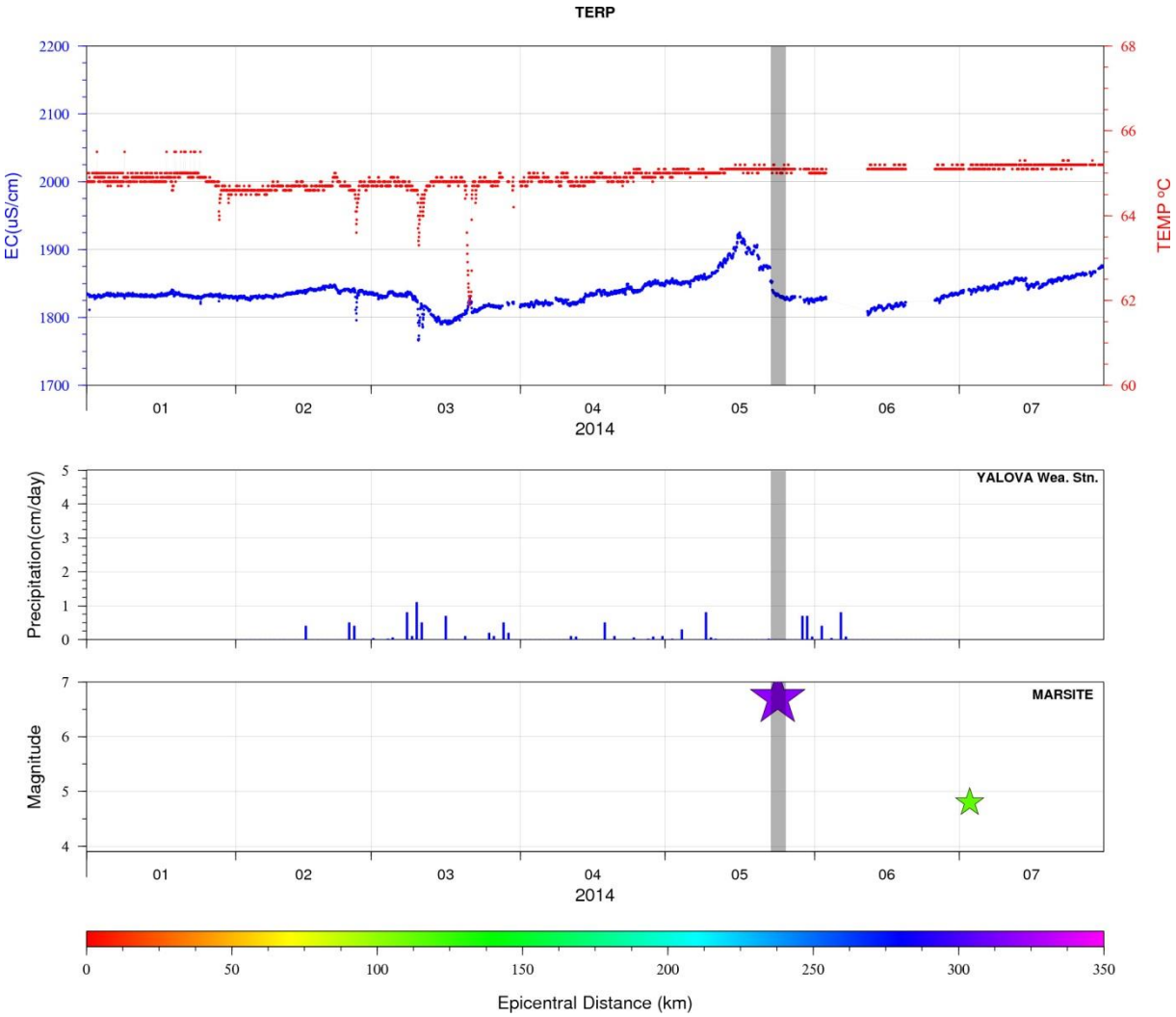

Figure 10 Detailed graph of TERP (Termal, Yalova) groundwater stations data. There is a electrical conductivity (EC) increase-decrease before the 24.05.2014, M=6.7 earthquakes, which occurred ~300 km west to the station. But there seems no anomaly before the 03.07.2014, M=4.8 earthquake, which occurred ~110 km southwest.

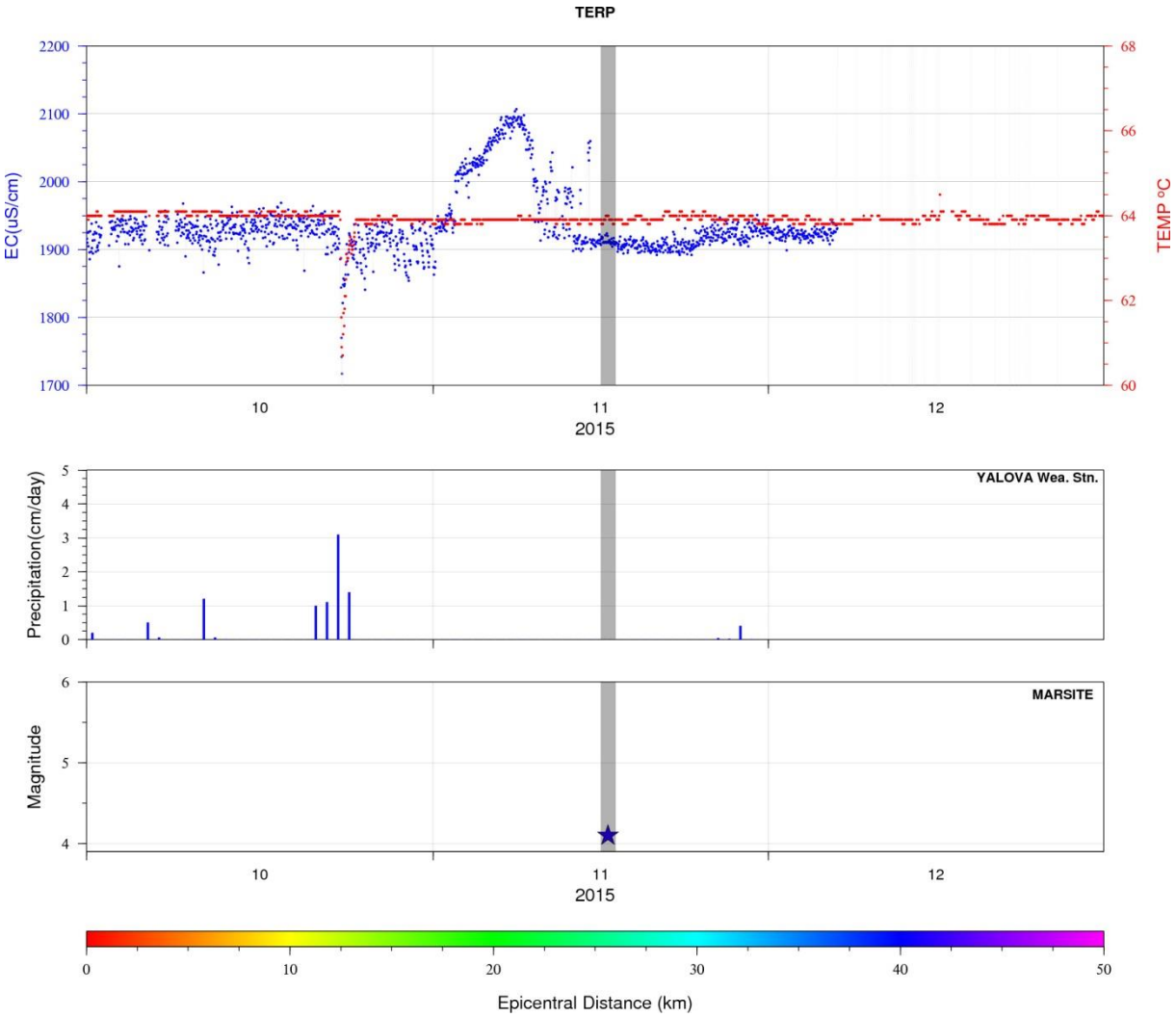

Figure 11 Detailed graph of TERP (Termal, Yalova) groundwater station data. There is a clear electrical conductivity (EC) increase-decrease before the 16.11.2015, M=4.1 earthquake, which occurred ~40 km northwest to the station.

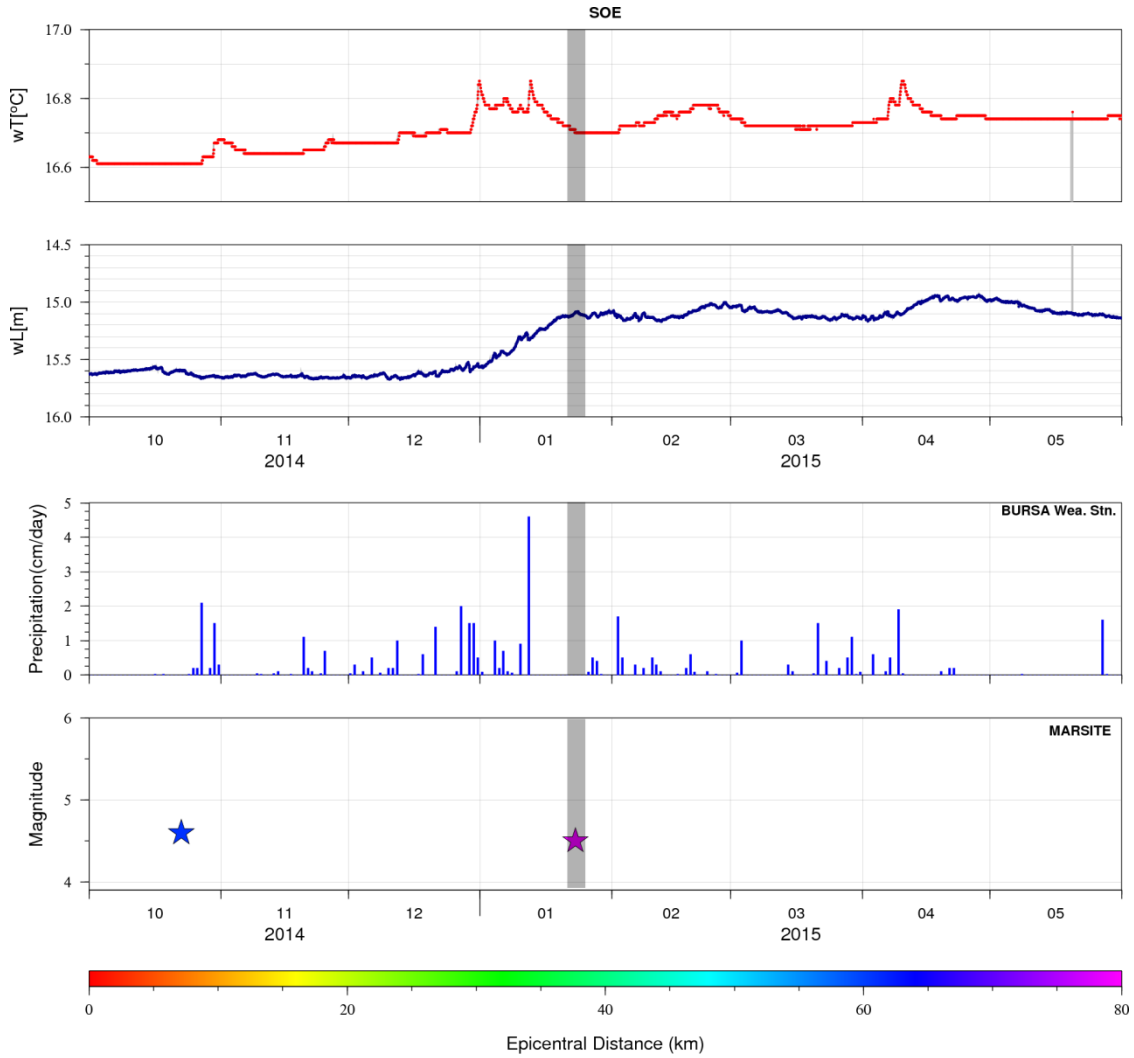

Figure 12- Detailed graph of SOE (Sölöz, Bursa) groundwater station data. No obvious anomalies were detected before the 22.10.2014, M=4.5 earthquake, which occur at ~60 km east to the station. But, there is a clear water temperature (wT) increase-decrease and water level (wL) increase before the 23.01.2015, M=4.5 earthquake (marked with grey strip), which occurred at ~80 km southwest to the station. During the station visit in 2015 a physical explanation for these positive temperature spikes emerged. There was a release of pressured gas while opening the wellhead. Thus, tentatively we propose that the rise of a giant gas bubble was responsible for the temperature spikes.

3 Circulation model

A possible circulation and interaction model can be proposed following Doglioni et al. (2014) who indicates the Brittle-Ductile-Transition (BDT) zone as the area that ideally separates two layers with different strain rates and structural styles. This behaviour determines a stress gradient that is eventually dissipated during the earthquake. The two layers also represent two fluid domains with different geochemical features. NAFZ-like strike-slip fault displays coexisting, locked and unlocked segments with opposite evolution (tension and shortening). During the interseismic period, they perform opposite evolutions (see *a* vs *b* on figure 13) inducing different behaviour in fluids circulation and changing both their geochemical features and flow rates.

Before the rupture the proportion of mantle fluids is expected to increase within the dilated band (figure 13, *a*) in contrast to an increased fluid expulsion over the shortened area. The contribution of mantle fluids over the same area might decrease during the coseismic period due to the enhancement of shallow

fluids expulsion induced by the sudden compression of the dilated band in figure 13, *a* due to the fault movement. The crustal relaxation of the brittle crust will result in an increase of the mantle fluids upraise over the newly formed dilated band (figure 13, *b*). Crustal deformation in dilating areas should be detectable by geodetic measurements.

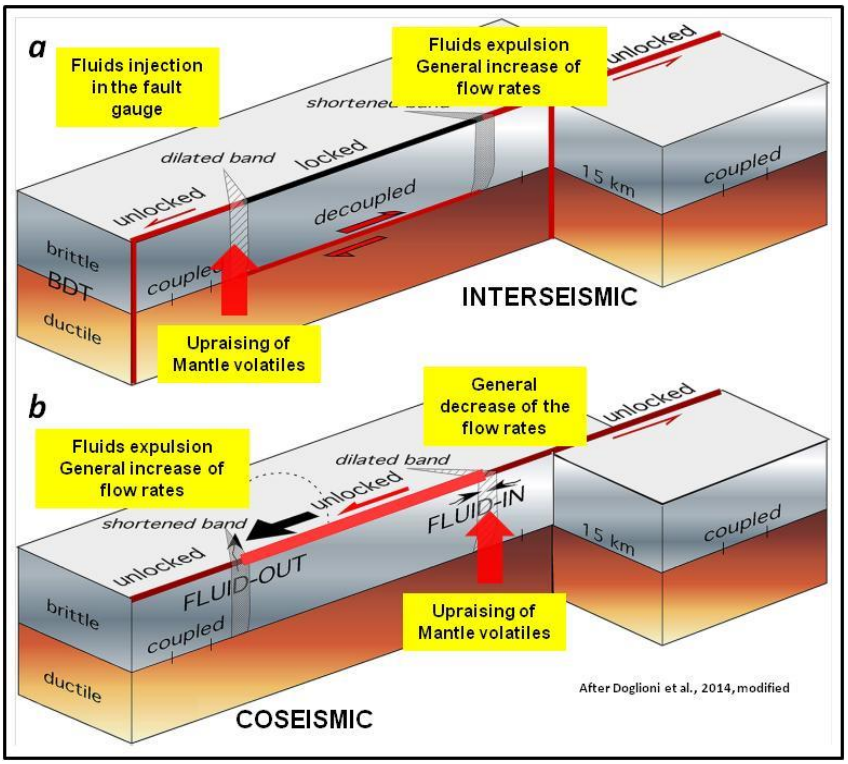

Figure 13– Schematic model of fluids circulation over segments of a seismogenic NAFZ-like strike-slip fault. Fluids of crustal and mantle origin mix in different proportions due to the different permeability in coincidence of areas undergoing dilatancy and compression as a function of their position to the respect of the locked fault planes. See text for details. Picture modified after Doglioni et al. (2014)

4 Conclusions

The results of the investigations carried out on the fluids vented over the area of the Sea of Marmara in the mainframe of the MARsite project allow us to highlight the geochemical features of the collected fluids and to constrain some processes responsible for their chemical and isotopic composition, including processes of mixings, fractionation as well as processes related to the fault activity as crustal deformation and rupture. The evidence that fluids originated in different domains interact and mix, leads to the conclusion that, over the Marmara area, crustal fluids are available along with mantle volatiles. The different geochemical features of the collected fluids (in terms of chemical and isotopic composition) associated to the evidence of an active natural degassing is a possible indication that different segments of the NAFZ cut crustal sections marked by variable geological and physical features (e.g. different rock types and permeability values). The composition of the circulating fluids is determined by the local geology (e.g. the hosting rocks where groundwaters equilibrate or interact with gases); however, in the case of contributions of mantle fluids it is necessary that fractures or faults cut the whole crustal thickness

allowing the volatiles of mantle origin to rise up and mix with crustal and other shallow fluids. In this case the composition of the deep fluids is a matter of tectonics.

As a matter of fact, since mantle degassing is not obvious in non-volcanic areas, we argue that high helium isotopic ratios and CO_2 degassing indicate the presence of mantle volatiles ascent through lithospheric faults. Evidence that fluids with a variable - sometimes significant - mantle component are vented over the whole Marmara region implies a widespread lithospheric character of the various NAFZ branches supporting the possibility of detecting changes in the fault behaviour from temporal and spatial changes in the mixing proportion of the deep and shallow fluid components.

5 References

Ambraseys. N. (2002). The seismic activity of the Marmara Sea region over the last 2000 years. Bull. Seismol. Soc. Am.. 92. 1–18.

Armijo. R.. Meyer. B.. Navarro. S.. King. G.. Barka. A.. 2002. Asymmetric slip partitioning in the Sea of Marmara pull-apart: a clue to propagation processes of the North Anatolian Fault? Terra Nova. 14(2): 80-86.

Armijo. R.. et al. (2005). Submarine fault scarps in the Sea of Marmara pull-apart (North Anatolian Fault): Implications for seismic hazard in Istanbul. Geochem. Geophys. Geosyst.. 6. Q06009. doi:10.1029/2004GC000896.

Barka. A. (1996). Slip distribution along the North Anatolian Fault associated with large earthquakes of the period 1939–1967. Seismol. Soc.Am. Bull.. 86. 1238–1254. Bonfanti P., Genzano N., Heinicke J., Italiano F., Martinelli G. , Pergola N., Telesca L., Tramutoli V. (2012) Evidences of CO2-gas emission variations in Central Apennines (Italy) during the L'Aquila seismic sequence (March-April 2009). Boll Geof.Teor. Appl., 53, 1, 147-168

Bohnhoff. M.. F. Bulut. G. Dresen. P. E. Malin. T. Eken. and M. Aktar (2013). An earthquake gap south of Istanbul. Nature. doi:10.1038/ncomms2999.

Bulut. F.. M. Bohnhoff. W. L. Ellsworth. M. Aktar and G. Dresen. (2009). Microseismicity at the North Anatolian Fault in the Sea of Marmara offshore Istanbul. NW Turkey. J. Geophys. Res. 114. B09302. doi:10.1029/2008JB006244.

Caracausi A., Italiano F., Martinelli G., Paonita A., Rizzo A. (2005) Long-term geochemical monitoring and extensive/compressive phenomena: case study of the Umbria region (Central Apennines, Italy). Annals of Geophysics, 48, 1, 43-53

Doglioni. C.. Barba. S.. Carminati. E.. Riguzzi. F.. (2011). Role of the brittle-ductile transition on fault activation. Physics of the Earth and Planetary Interiors 184. 160-171. http://dx.doi.org/10.1016/j.pepi.2010.11.005.

Doglioni. C.. Barba. S.. Carminati. E.. Riguzzi. F.. 2014. Fault on–off versus coseismic fluids reaction. Geoscience Frontiers. 5(6): 767-780.

Ergintav. S.. S. McClusky. E. Hearn. R. Reilinger. R. Cakmak. T. Herring. H. Ozener. O. Lenk. and E. Tari (2009). Seven years of postseismic deformation following the 1999. M = 7.4 and M = 7.2 Izmit-Duzce. Turkey earthquake sequence. J. Geophys. Res.. 114. B07403. doi:10.1029/2008JB006021.

Ergintav S.. Reilinger R. E.. Çakmak R.. Floyd M.. Çakır Z.. Doğan U.. King R. W.. McClusky S.. and Özener H. (2014) Istanbul's earthquake hot spots: Geodetic constraints on strain accumulation along faults in the Marmara seismic gap. Geophysical Research Letters. 41(16): 5783-5788.

Faure. G.. (1986). Principles of isotope geology. Wiley New York. 2nd Edition. pp. 589.

Flerit. F.. Armijo. R.. King. G.C.P.. Meyer. B.. Barka. A.. 2003. Slip partitioning in the Sea of Marmara pull-apart determined from GPS velocity vectors. Geophysical Journal International. 154(1): 1-7.

Gasperini L., Polonia A., Del Bianco F., Etiope G., Marinaro G., Italiano F., Favali P., N.M. Cagatay, López-García P. (2012) Gas seepages and seismogenic structures along the North Anatolian Fault in the Eastern Marmara Sea. G-Cubed, vol 13-10, doi:10.1029/2012GC004190

Giggenbach. W. F. (1988). Geothermal solute equilibria. derivation of Na-K-Mg-Ca geoindicators. *Geochimica et Cosmochimica Acta*. *52*(12). 2749-2765.

Hartmann. J.. Levy. J.K.. 2005. Hydrogeological and gasgeochemical earthquake precursors - A review for application. Natural Hazards. 34(3): 279-304.

Heinicke. J.. U. Koch. and G. Martinelli (1995). CO2 and radon measurements in the Vogtland area (Germany) - a contribution to earthquake prediction research. *Geophysical Research Letters*. *22*(7). 771-774.

Heinicke. J.. Braun. T.. Burgassi. P.. Italiano. F.. Martinelli. G.. 2006. Gas flow anomalies in seismogenic zones in the Upper Tiber Valley. Central Italy. Geophysical Journal International. 167(2): 794-806.

Heinicke J., F. Italiano, U. Koch, G.Martinelli and L. Telesca (2010) Anomalous fluid emission of a deep borehole in a seismically active area of Northern Apennines (Italy) App. Geochem., 25, 4, 555-571, doi : 10.1016/j.apgeochem.2010.01.012

Hilton. D.R.. 1996. The helium and carbon isotope systematics of a continental geothermal system: results from monitoring studies at Long Valley caldera (California. USA). Chemical Geology. 127(4): 269-295.

Hilton. D.R.. 2007. Geochemistry. The leaking mantle. Science. 318(5855): 1389-90.

Holocher J. Peeters F. Aeschbach-Hertig W. Hofer M. Brennwald M.. Kinzelbach W.. Kipfer R.. (2002) Experimental investigations on the formation of excess air in quasi-saturated porous media. Geochimica et Cosmochimica Acta. 66. 23. 4103–4117

Inan. S.. T. Akgül. C. Seyis. R. Saatçılar. S. Baykut. S. Ergintav. and M. Baş (2008). Geochemical monitoring in the Marmara region (NW Turkey): A search for precursors of seismic activity. *Journal of Geophysical Research*. *113*(B3). B03401. doi:10.1029/2007JB005206.

Ingebritsen. S.E.. Manga. M.. 2014. Earthquakes: Hydrogeochemical precursors. Nature Geoscience. 7(10): 697-698.

Italiano F.. Martelli M.. Martinelli G.. Nuccio P.M. (2000) Geochemical evidences of melt intrusions along lithospheric faults of Irpinian Apennines (Southern Italy): Geodynamic and seismogenetic implications. Jour. Geoph. Res.. 105. B6. 13569-13578

Italiano, F.; Martinelli, G.; Nuccio, P. M. (2001). Anomalies of mantle-derived helium during the 1997-1998 seismic swarm of Umbria-Marche, Italy Geophys. Res. Lett. Vol. 28 , No. 5 , p. 839-842

Italiano F., Martinelli G., Rizzo A. (2004) Geochemical evidence of seismogenic-induced anomalies in the dissolved gases of thermal waters: A case study of Umbria (Central Apennines, Italy) both during and after the 1997–1998 seismic swarm. G-Cubed, vol. 5, 11, doi:10.1029/2004GC000720

Italiano F., Caracausi A., Favara R., Innocenzi P., Martinelli G. (2005) Geochemical monitoring of cold waters during seismicity: implications for earthquake-induced modification in shallow aquifers, Terrestrial and Atmospheric and Oceanic Sciences, 16, 4, 709-729

Italiano. F.. Martinelli. G.. Plescia. P.. (2008). CO2 degassing over seismic areas: the role of mechanochemical production at the study case of Central Apennines. Pageoph. 165. 1. 75-94.

Italiano F.. Bonfanti P.. Ditta M.. Petrini R.. Slejko F. (2009) Helium and carbon isotopes in the dissolved gases of Friuli Region (NE Italy): Geochemical evidence of CO2 production and degassing over a seismically active area. Chemical Geology. 266 (1-2) 76-85. doi: 10.1016/j.chemgeo.2009.05.022

Italiano F., Martinelli G., Bonfanti P., Caracausi A. (2009) Long-term geochemical monitoring of gases from the seismic area of the Umbria region: 1997-2007. Tectonophysics, 476 (2009) 282–296

Italiano F., Bonfanti P., Pizzino L., Quattrocchi F. (2010) Fluids-Faults relationships over the seismic area of Southern Apennine (Calabria region, Southern Italy): geochemical information from thermal and sulphurous water discharges. App. Geochem., 25, 4, 540-554, doi: 10.1016/j.apgeochem.2010.01.011

Italiano F.. Sasmaz A.. Yuce G.. Okan O. (2013) Thermal fluids along the East Anatolian Fault Zone (EAFZ): geochemical features and relationships with the tectonic setting. Chemical Geology. 339. 103-114. doi.org/10.1016/j.chemgeo.2012.07.027

Italiano F.. Yuce G.. Uysal I.T.. Gasparon M.. Morelli G. (2014) Insights into mantle-type volatiles contribution from dissolved gases in artesian waters of the Great Artesian Basin. Australia. Chemical Geology. Volumes 378–379. 15 June 2014. pp. 75-88. ISSN 0009-2541. http://dx.doi.org/10.1016/j.chemgeo.2014.04.013.

Javoy. M.. Pineau. F.. Delorme. H.. 1986. Carbon and nitrogen isotopes in the mantle. Chem. Geol. 57 (1-2). 41-62.

Karabulut. H.. M.-P. Bouin. M. Bouchon. M. Dietrich. C. Cornou. and M. Aktar (2002). The seismicity of the eastern Marmara Sea after the 17 August 1999 Izmit earthquake. Bull. Seismol. Soc. Am.. 92. 387–393.

Karabulut. H.. J. Schmittbuhl. S. Özalaybey. O. Lengliné. A. Kömeç-Mutlu. V. Durand. M. Bouchon. G. Daniel. and M. P. Bouin (2011). Evolution of the seismicity in the eastern Marmara Sea a decade before and after the 17 August 1999 Izmit earthquake. Tectonophysics. 510. 17–27.

Le Pichon. X.. A. M. C. Sengor. E. Demirbag. C. Rangin. C. Imren. R. Armijo. N. Gorur. and N. Cagatay (2001). The active Main Marmara Fault. Earth Planet. Sci. Lett.. 192. 595–616.

Le Pichon. X.. N. Rangin. C. Chamot-Rooke. and A. M. C. Sengör (2003). The North Anatolian Fault in the Sea of Marmara. J. Geophys. Res..108(B4). 2179. doi:10.1029/2002JB001862.

Mamyrin. B. A.. Tolstikhin. I. N.. (1984). Helium Isotopes in Nature. Elsevier. New York.

McHugh. C. M. G.. N. Braudy. M. N. Çağatay. C. Sorlien. M.-H. Cormier. L. Seeber. and P. Henry (2014). Seafloor fault ruptures along the North Anatolia Fault in the Marmara Sea. Turkey: Link with the adjacent basin turbidite record. Mar. Geol.. 353. 65–83.

Meade. B. J.. B. H. Hager. S. C. McClusky. R. E. Reilinger. S. Ergintav. O. Lenk. A. Barka. and H. Ozener (2002). Estimates of seismic potential in the Marmara region from block models of secular deformation constrained by GPS measurements. Bull. Seismol. Soc. Am.. 92. 208–215.

Mogi. K.. Mochizuki. H.. Kurokawa. Y.. 1989. Temperature changes in an artesian spring at Usami in the Izu Peninsula (Japan) and their relation to earthquakes. Tectonophysics. 159(1-2): 95-108.

Mutlu. H.. Gulec. N.. Hilton. D.R.. Aydin. H.. Halldorsson. S.A.. 2012. Spatial variations in gas and stable isotope compositions of thermal fluids around Lake Van: Implications for crust-mantle dynamics in eastern Turkey. Chemical Geology. 300: 165-176.

Norman. J. M.. Garcia R.. and Verma S. B.. 1992. Soil surface CO_2 fluxes and the carbon budget of a grassland. J. Geophys. Res.. 97. 18.845–18.853. doi:10.1029/92JD01348.

Norman. J. M.. Kucharik C. J.. Gower S. T.. Baldocchi D. D.. Crill P. M.. Rayment M.. Savage K.. and Striegl R. G.. 1997. A comparison of six methods for measuring soil–surface carbon dioxide fluxes. J. Geophys. Res.. 102. 28.771–28.777. doi:10.1029/97JD01440.

Ozima. M.. Podosek. F. A.. 2002. Noble Gas Geochemistry. 2nd ed.. Cambridge University Press. 286 pp.

Parsons. T. (2004). Recalculated probability of M 7 earthquakes beneath the Sea of Marmara. Turkey. J. Geophys. Res.. 109. B05304.doi:10.1029/2003JB002667.

Perrier. F.. et al. (2009). A direct evidence for high carbon dioxide and radon-222 discharge in Central Nepal. *Earth and Planetary Science Letters*. *278*(3-4). 198-207. doi:10.1016/j.epsl.2008.12.008.

Petrini R., F. Italiano, A. Riggio, F.F. Slejko, M. Santulin, A. Buccianti, P. Bonfanti And D. Slejko (2012) Coupling geochemical and geophysical signatures to constrain strain changes along thrust faults. Boll Geof.Teor. Appl., Vol. 53, 1, 113-134. DOI: 10.4430/bgta0017

Pondard. N.. R. Armijo. G. C. P. King. B. Meyer. and F. Flerit (2007). Fault interactions in the Sea of Marmara pull-apart (North Anatolian Fault):Earthquake clustering and propagating earthquake sequences. Geophys. J. Int.. 171(3). 1185–1197.

Roeloffs. E.. Quilty. E.. 1997. Case 21 water level and strain changes preceding and following the August 4. 1985 Kettleman Hills. California. earthquake. Pure and Applied Geophysics. 149(1): 21-60.

Sano. Y.. Wakita. H.. 1988. Precise measurement of helium isotopes in terrestrial gases. B. Chem. Soc. Jpn. 61. 1153–1157.

Sano. Y.. Marty. B.. 1995. Origin of carbon in fumarolic gas from island arc. Chem. Geol. 119. 265–74.

Sibson. R.H.. 1992. Implications of fault-valve behaviour for rupture nucleation and recurrence. Tectonophysics. 211(1-4): 283-293.

Sinclair. A.J.. 1991: A fundamental approach to threshold estimation in exploration geochemistry: Probability plots revisited. J. Geochem. Explor.. 41. (1991). 1– 22.

Singh. A.K. and Engelhardt. M.. 1997. The lognormal distribution in environmental applications. EPA/600/R-97/066. Environmental Protection Agency. Washington. DC.

Skelton. A. et al.. 2014. Changes in groundwater chemistry before two consecutive earthquakes in Iceland. Nature Geoscience. 7(10): 752-756.

Stein. R. S.. A. Barka. and J. D. Dieterich (1997). Progressive failure on the North Anatolian fault since 1939 by earthquake stress triggering. Geophys. J. Int.. 128. 594–604.

Steinitz. G.. O. Piatibratova. and U. Malik (2015). Observations on the spatio-temporal patterns of radon along the western fault of the Dead Sea Transform. NW Dead Sea. *EPJST*. *(in press)*.

Tan. O.. M. C. Tapırdamaz. and A. Yörük (2008). The earthquake catalogues for Turkey. Turkish J. Earth Sci.. 17. 405–418.

Toutain. J.P.. Baubron. J.C.. 1999. Gas geochemistry and seismotectonics: a review. Tectonophysics. 304(1-2): 1-27.

Tunc. B.. et al. (2011). The Armutlu Network: an investigation into the seismotectonic setting of Armutlu-Yalova-Gemlik and the surrounding regions. *Annals of Geophysics*. *54*(1). 35-45. doi:10.4401/Ag-4877.

van Geldern. R.. M. E. Nowak. M. Zimmer. A. Szizybalski. A. Myrttinen. J. A. C. Barth. and H.-J. Jost (2014). Field-Based Stable Isotope Analysis of Carbon Dioxide by Mid-Infrared Laser Spectroscopy for Carbon Capture and Storage Monitoring. *Analytical Chemistry*. *86*(24). 12191-12198. doi:10.1021/ac5031732.

Wakita. H.. 1981. Precursory changes in groundwater prior to the 1978 Izu-Oshima- Kinkai earthquake. Earthquake Prediction - An International Review. Maurice Ewing Series. pp. 527-532.

Wang. C.-y.. Manga. M.. 2010. Earthquakes and water. Lecture notes in earth sciences 114. Springer. Berlin-Heidelberg.

Weinlich. F. H.. E. Faber. A. Bouskova. J. Horalek. M. Teschner. and J. Poggenburg (2006). Seismically induced variations in Marianske Lazne fault gas composition in the NW Bohemian swarm quake region. Czech Republic - A continuous gas monitoring. *Tectonophysics*. *421*(1-2). 89-110. doi:10.1016/j.tecto.2006.04.012.

Weiss. R.F.. 1974. Carbon dioxide in water and seawater: the solubility of a non-ideal gas. Marine Chemistry. 2(3): 203-215.

Wiersberg. T.. S. Suer. N. Gulec. J. Erzinger. and M. Parlaktuna (2011). Noble gas isotopes and the chemical composition of geothermal gases from the eastern part of the Buyuk Menderes Graben (Turkey). *Journal of Volcanology and Geothermal Research*. *208*(3-4). 112-121. doi:DOI 10.1016/j.jvolgeores.2011.09.009.

Werner. C.. Brantley. S.L.. and Boomer. K.. 2000. CO_2 emissions related to the Yellowstone volcanic system. 2. Statistical sampling. total degassing. and transport mechanisms. J. Geophys. Res.. 105. (B5). 10831–10846.

Toutain. J. P.. M. Munoz. J. L. Pinaud. S. Levet. M. Sylvander. A. Rigo. and J. Escalier (2006). Modelling the mixing function to constrain coseismic hydrochemical effects: An example from the French Pyrenees. *Pure and Applied Geophysics*. *163*(4). 723-744.

Woith. H.. et al. (2000). Multidisciplinary investigations of the German Task Force for Earthquakes related to the Izmit earthquake of August 17. 1999 and the Düzce earthquake of November 12. 1999. in *The 1999 Izmit and Düzce Earthquakes: preliminary results*. edited by A. Barka. Ö. Kozaci. S. Ayküz and E. Altunel. pp. 233-245. Istanbul Technical University. Istanbul.

Woith. H. et al.. 2003. Heterogeneous response of hydrogeological systems to the Izmit and Duzce (Turkey) earthquakes of 1999. Hydrogeology Journal. 11(1): 113-121.

Woith. H.. A. P. Venedikov. C. Milkereit. M. Parlaktuna. and A. Pekdeger (2006). Observation of crustal deformation by means of wellhead pressure monitoring. *Bulletin d'Information des Marees Terrestres*. *141*. 11277-11285.

Woith. H.. 2015. Radon earthquake precursor: A short review. The European Physical Journal Special Topics. 224(4): 611-627.

Wyss. M. (1991). *Evaluation of proposed earthquake precursors*. 94 pp.. American Geophysical Union. Washington D.C.

Yan. R.. H. Woith. and R. Wang (2014). Groundwater level changes induced by the 2011 Tohoku earthquake in China mainland. *Geophysical Journal International*. *199*(1). 533-548

Zmazek B., F. Italiano, J. M. Živčić, Vaupotič, I. Kobal, G. Martinelli. (2002) Geochemical monitoring of thermal waters in Slovenia: relationships to seismic activity. Applied Radiation and Isotopes, 57/6, 919-930